

value of the incentive payments may be higher than a potential claim, it is a predictable value that the owner can include in the project budget.

An additional advantage of the incentive provision approach is to avoid the difficulties in determining if a DSC has been encountered. As noted above, boulders are one of the biggest risks to the project. In a typical GBR, the boulder risk would be presented as a baseline number and strength of boulders. However, during mining with a MTBM, the boulders are crushed before being ingested by the machine, making it almost impossible to determine if a boulder has been encountered. Similarly, the soils encountered during mining with a MTBM cannot be directly observed, and the density of the ground must be inferred from the MTBM operational parameters and the material coming off of the slurry separation plant, which has been thoroughly remixed during transport to the surface.

Once the decision was made to pursue the incentive provision, the design team began focusing on the details of such a provision. Primarily, the amount of the incentive needed to be established, along with the timeframe in which the mining needed to be completed in order to collect the full incentive payment. Additionally, a limited number of baselines would be provided in the specifications; however, the nature of these baselines needed to be established.

In order for the incentive payment to be an effective risk reduction tool, the amount of the payment had to be higher than the probable value of a DSC claim. It was not intended to cover the cost of a major difficulty, such as a stuck MTBM. Since this was a new approach to baselining a microtunnel project, no guidance for sizing this payment had been previously established. However, the project team understood that the payment had to hold enough value to be worth more to a contractor than a potential DSC. The project team discussed their experiences with local microtunneling projects and established a typical range of the monetary cost of DSC claims on various local projects. They then established a level of risk tolerance that the owner was willing to accept. In this case, the project team estimated that an incentive payment equal to approximately 2% of the engineer's estimate for the project was appropriate and put an incentive payment of \$250,000 per microtunnel drive (\$500,000 total) into the specifications.

In order to collect the incentive payment, the contractor would have to complete each drive within a specified timeframe. The project team used a similar approach to determine this timeframe by discussing experiences on recent local projects and establishing a range of typical mining rates. The goal was to select a timeframe that was readily achievable by an experienced microtunnelling contractor, but not overly conservative. In this case, the team selected 75 hours of mining time to complete each of the drives, which corresponds to an average rate of mining equal to 1.88 meters/hour (6.19 feet/hour). As a part of this process, it was important to include in the specifications a definition of mining time that was readily measurable during construction. The team defining mining time as time in which one of the following conditions were met:

1. The MTBM cutterhead is rotating and forward progress of the MTBM is being achieved, or;
2. The pipe jacking system is in operation progressing the microtunnel forward; or
3. The cutterhead of the microtunnel is being withdrawn to allow progressing of the microtunnel.

In order to provide some guidance to the contractor in the selection of equipment, means, and methods to advance the microtunnel, some baseline information was provided in the specifications. This baseline information was limited to the maximum size of boulders to be encountered, the maximum strength of the boulders to be encountered, and the abrasivity of the ground. The specifications specifically noted that gravel, cobbles, and boulders up to 42-inches

in maximum dimension would be encountered in the microtunnel drive with no limit on the quantities of each. The GDR, which included boring logs and laboratory test data collected for the project, was also included as a contract document.

Additionally, the specifications included requirements for the MTBM equipment. The MTBM was required to be a new, slurry pressure balance shield type MTBM. More specifically, a minimum drive power of 200kW was specified, disc cutters were required, and a maximum cutterhead opening ratio of 25% was included in the specified requirements. Additionally, the contractor was required to submit a report on the condition of the machine after the first drive, and new tools were required for the second drive. These provisions were included to reduce the risk that the disc cutters would not break up any encountered boulders, clogging the cutterhead with large fragments.



**Figure 2. MTBM Face Before (Left) and After (Right) First Microtunnel Drive**

## EXECUTION OF CONTRACT

The contract for the construction of the project was awarded to Stellar J Construction based on their low bid. Competition for the project was strong, with the winning bid coming in approximately 12.6% below the engineer's estimate, and only 0.13% below the next lowest bid. Construction on the site began in April 2015, and the microtunnel drives were completed during April and May of 2016 (first drive) and June and July of 2016 (second drive).

The first drive was mined to completion in 82.0 hours of mining time, earning the contractor the full incentive payment. During the launch of the MTBM, a faulty weld resulted in groundwater leakage into the MTBM main bearing housing. The MTBM manufacturer repaired this defect, but the launch of the MTBM was delayed by approximately two months. However, once mining started, no unanticipated conditions were encountered during the first drive. Upon retrieval of the MTBM at the completion of the first drive, the contractor noted that one disc cutter had worn significantly, resulting in two flat spots on the disc itself, and a series of grooves worn into the surrounding buckets. Figure 2 shows the condition of the face before and after the

first microtunnel drive The contractor replaced all of the tooling and re-hardfaced the face prior to the launch of the second drive.

The second drive was mined to completion in 56.5 hours of mining time, also earning the contractor the full incentive payment. On this drive, unanticipated conditions were encountered. While passing under the south bank of the LWSC, manmade objects were found in the spoils, as shown in Figure 3. These objects indicated that the microtunnel passed through a recent soil deposit, and not the glacially overconsolidated glacial till that was anticipated in this area.



**Figure 3. Manmade Debris Encountered in Second Microtunnel Drive**



**Figure 4. Cutterhead upon Completion of the Second Microtunnel Drive**

The contractor submitted a DSC notice upon encountering this debris. However, the impact of the unanticipated condition was minimal, so the contractor chose not to pursue a RCO which

would have nullified the incentive payment.

Wear on the face of the MTBM was significantly less than that noted during the first drive. One of the center disc cutters was slightly flatspotted, but no other significant wear was observed. Figure 4 shows the condition of the cutterhead upon completion of the second drive.

## LESSONS LEARNED

Overall, the microtunneling portion of the Fremont Siphon Replacement Project was a successful endeavor. Unanticipated conditions were encountered one time, but no RCO was submitted. Both microtunnel drives were completed within the specified timeframes, earning the contractor two complete incentive payments.

One significant lesson learned from the project was that the definition of mining time is critical. Although a definition was provided in the specifications, the contractor and the owner had slightly different views on the interpretation of that definition. For future projects, we recommend tightening the language in the definition of mining time or allowing the resident engineer the freedom to negotiate with the contractor during the project start-up phase and requiring the contractor to include their intended procedure for counting mining time to be included in the microtunneling plan submittal early on in the project.

Due to the success of this project, a similar approach has now been utilized on the Ship Canal Water Quality Project (SCWQP), which also includes a microtunnel portion beneath the LWSC. The SCWQP design team felt that the incentive amount of \$250,000 per drive use on the Fremont Siphon Replacement was appropriate and maintained that value for the single drive of the SCWQP microtunnel.

For microtunnel projects in complex glacial geology, the use of a typical GBR can lead to unexpected risks. By limiting the amount of difficult to measure baseline information provided and including an incentive provision that precludes the submittal of frivolous RCOs, this risk can be managed effectively to the benefit of all contracted parties.

## REFERENCES

- ASCE. (2007). *Geotechnical Baseline Reports for Construction: Suggested Guidelines*. Essex, Randall J., ed. Reston, VA.
- Yount, J.C., Dembroff, G.R., and G.M. Barats. (1985). *Map Showing Depth to Bedrock in the Seattle 30' by 60' Quadrangle, Washington*. U.S. Geological Survey Map MF-1692.

## Evaluation of the Efficiency of the Umbrella Arch Method in Urban Tunneling Subjected to Adjacent Surcharge Loads

Ali Morovatdar, S.M.ASCE<sup>1</sup>; Massoud Palassi<sup>2</sup>; and Mahsa Beizaei<sup>3</sup>

<sup>1</sup>Graduate Research Assistant, School of Engineering, Dept. of Civil Engineering, Univ. of Tehran, Tehran, Iran. E-mail: alimoro6900@gmail.com

<sup>2</sup>Associate Professor, School of Engineering, Dept. of Civil Engineering, Univ. of Tehran, Tehran, Iran. E-mail: mpalass@ut.ac.ir

<sup>3</sup>Ph.D. Research Associate, Dept. of Civil Engineering, Univ. of Texas at El Paso, El Paso, TX. E-mail: mbeizaei@miners.utep.edu

### ABSTRACT

Since urban tunnels constructed in the weak ground at shallow depth are highly sensitive to the stress level, surcharge loads resulting from adjacent buildings can dramatically increase the induced stresses and settlements, and even failure of the buildings can take place. In this study, utilizing three-dimensional finite element models, the efficiency of the umbrella arch method (UAM) on stabilizing the tunnels subjected to the surcharge loading is investigated. The analysis considers the actual field conditions of implementing the UAM and the primary supporting system. For the surcharge loads applied in this study, the analysis results showed that using the UAM can efficiently control the tunnel crown and ground surface settlements by at least 48% and 33%, respectively. Consequently, reinforcing the tunnels using UAM is one of the effective ways to overcome the severe conditions, in terms of safety and stability, in urban tunneling under existing adjacent buildings.

### INTRODUCTION

Considering the drastic changes in urban development, tunneling in urban areas is one of the most effective solution alternatives to address inner-city transportation problems. However, urban tunnels are mostly located under adjacent buildings in densely populated areas. For these critical regions, constructing the tunnel without causing any damage to the buildings is of highest importance. Particularly, in the case of tunneling in weak and shallow ground, which is common in urban areas, the ground settlement is the most significant factor that can seriously damage buildings (Beyzaei and Seyedi Hosseininia 2019). Hence, one of the main challenges for engineers in urban tunneling is to limit surface settlements to acceptable ranges. This is extremely important not only from the tunnel stability viewpoint but also due to the potential damage to adjacent buildings.

Tunnel excavation deploying New Austrian Tunneling Method (NATM), in combination with auxiliary supporting techniques, is becoming common to overcome the significant difficulties encountered while tunneling in urban areas. Several reinforcement techniques such as Umbrella Arch Method (UAM), jet grouting, mechanical pre-cutting, and sub-horizontal fiber glass reinforcement have been deployed in urban areas to limit the tunnel excavation-induced settlements. Specifically, UAM has been used to a great extent, due to its potential pre-reinforcement capabilities (Song et al. 2013). In this approach, prior to tunnel excavation, a series of forepoling pipes are installed along the tunnel circumference in the crown. Subsequently, by injecting the grout through the pipes, the stiffened soil (between the pipes) and the forepoling pipes create an umbrella-shaped arch above the tunnel. This arrangement

considerably enhances the stiffness properties of the impacted soil and improves the tunnel excavation stability. Tunneling procedure using pre-reinforcement UAM is well explained in the literature by Yoo and Shin (2003), Ocaik (2008), Aksoy and Onargan (2010), and Klotoé and Bourgeois (2019).

Several experimental and numerical studies have been conducted to investigate the performance of the umbrella arch method in the tunnel construction procedure. Ocaik (2008) studied second stage excavation of Istanbul Metro, which was constructed using NATM in combination with UAM and resulted that using this technique can effectively control the surface deformations, especially in clay-bearing formations. Aksoy and Onargan (2010) assessed the influence of implementing UAM and tunnel face bolts on ground surface settlements induced during the tunnel construction of 2nd phase of Izmir Metro, which was located in the densely populated district. The results of numerical modeling indicated that the UAM and face bolt applications could considerably reduce the risk of buildings' failure by decreasing the ground settlements by 69%. Yoo and Shin (2003) conducted laboratory and numerical studies on the deformation behavior of tunnel face supported by longitudinal pipes. The results showed that face reinforcing technique could efficiently control the ground settlements during urban tunneling. Shin et al. (2008), deploying a large-scale model, investigated the UAM reinforcing mechanism in granular soils. They also studied the effect of pipe length on the tunnel stability and found that the pipe reinforcement of heading can significantly improve the tunnel face stability. Hisatake and Ohno (2008) conducted centrifugal model tests to evaluate the effect of using UAM on tunnel displacements reduction. They found that deploying the pipe roof supports can decrease the ground displacements by 75%.

Finite Element (FE) and finite difference methods have been widely utilized to assess the performance of in-service infrastructures such as tunnels, roadway, bridges, foundations, and levees (Morovatdar et al. 2019, 2020a; Abadi et al. 2015; Rahimi et al. 2019). These methods have also been employed to evaluate different aspects of the UAM as a tunnel reinforcement technique. Song et al. (2013) developed a finite element software to evaluate various conditions and variables of the UAM. The developed model was instrumental in estimating the quantity of forepoling steel pipes needed for the UAM at an early stage of the tunnel design protocol. Oke et al. (2014), using 2D and 3D models, investigated how numerical modeling can be implemented as an effective tool to evaluate the influential design parameters attributed to the use of the UAM technique. Recently, Klotoé and Bourgeois (2019), conducting 3D finite element simulations, evaluated the influence of the UAM on the settlements induced by shallow tunneling. The authors found that the influence of using the UAM on the settlements remained modest for the range of parameters considered in the analysis.

Previous studies in the literature have provided insights into the working mechanism and behavior of the tunnel reinforced by the umbrella arch technique. However, the majority of these studies have been concentrated on general practices of the UAM with several simplifications made in the analysis. In some numerical analyses, the UAM elements (steel pipes, grout, and soilcrete) were simulated as one single element with equivalent material properties based on the weighted averages. Making such simplifications, instead of modeling the UAM elements individually, simulates the circumstance that is vastly different from the actual field conditions, and hence, it can seriously jeopardize the accuracy of the analysis results (Morovatdar et al. 2020b). Furthermore, limited number of studies were focused on quantification of the UAM impacts on stabilizing the urban tunnels subjected to adjacent buildings.

In addition to the aforementioned limits, lack of a uniform and standardized guideline to

evaluate the effect of using UAM in urban tunneling resulted in widespread and even contradicting approach. Therefore, the influence of UAM on urban tunneling still needs to be investigated and quantified to improve the existing knowledge associated with this technique. In this study, using a series of 3D finite element models, the efficiency of using the umbrella arch method on stabilizing the urban tunnels subjected to the various surcharge loadings was investigated. This practical investigation considered the actual field conditions of tunnel construction procedure, and UAM deployment, based on the information gathered from Tohid tunnel project.

## RESEARCH METHODOLOGY

In this study, tunnel excavation procedure was simulated in ABAQUS finite element software, considering two different conditions; using the pre-support UAM technique, and also without using it. It should be noted that the tunnel construction procedure was adopted based on the detailed information gathered from Tohid Tunnel project, constructed in Tehran (Iran). This information was a direct input to the FE analysis to more accurately simulate the actual field conditions. Subsequently, three different surcharge loads (in different relative location to the tunnel axis orientation), associated with the adjacent buildings, were applied to the simulated models to properly evaluate the efficiency of using the UAM in stability improvement of the tunnel in various situations. Ultimately, induced tunnel crown and ground surface settlements were calculated for further comparative analysis. Comprehensive information regarding the finite element models, tunnel excavation procedure, and UAM deployment is provided in the subsequent sections.

### Numerical Modeling Simulation

#### Model Dimension

Proper characterization of the dimensions and geometry of the model are of utmost importance to mitigate the systematic errors associated with boundary effect problems. The authors carried out a comprehensive sensitivity analysis to determine the adequate model dimensions for simulation purposes. It was found that the sensitivity of the tunnel crown settlement was negligible when the simulated model dimensions exceed 50, 50, and 70 meters for height, width, and length of the model, correspondingly. Therefore, a 3D soil block with dimensions of 50×50×70 m was modeled in ABAQUS using continuum rigid elements, as shown in Figure 1.

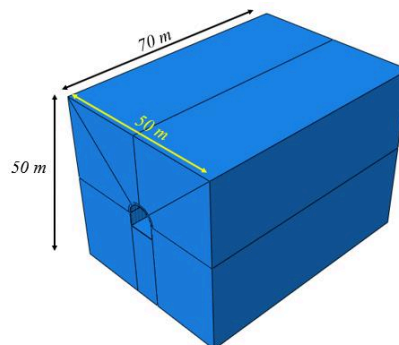


**Figure 1. Simulated soil block in ABAQUS.**

## Geometric Properties of the Simulated Tunnel

Tohid tunnel was constructed in Tehran in 2014. This arch-shaped tunnel with a height and width of 8 m, is categorized as highway tunnels in urban areas. Geometric properties of the tunnel were incorporated into the finite element simulation, which is tabulated in Table 1.

**Table 1. Geometric Properties of Tohid Tunnel (Tehran)**

| Geometric Characterization | Quantity |
|----------------------------|----------|
| Length                     | 1800 m   |
| Longitudinal slope         | -1.14%   |
| Maximum overburden height  | 20 m     |
| Tunnel span                | 8 m      |
| Tunnel height              | 8 m      |

## Primary Supporting System

The tunnel was excavated using the New Austrian Tunneling Method (NATM). In this approach, the primary supporting system consisted of steel frames and shotcrete. These components with the assigned dimensions were simulated in the software, as shown in Figure 2. The tunnel construction process was followed by one-meter excavation steps. After each excavation steps, steel sets were modeled by wire elements in the tunnel with one-meter longitudinal distances, and then the tunnel excavation face, tunnel wall, and the tunnel invert were covered by shotcrete shell elements. It should be noted that the supporting system in the deployed NATM was comprised of 20 cm shotcrete and IPE18 as the steel sets.

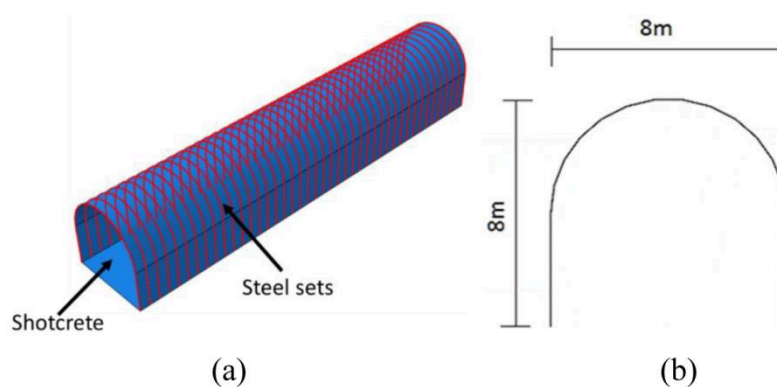


**Figure 2. Primary supporting system components, (a) 3D model, (b) dimensions of the model.**

## Deploying the Umbrella Arch Method

Prior to the tunnel excavation initiation, based on the field testing and laboratory investigation, it was found that the existing soil around the tunnel was relatively weak. Essentially, the most portion of the tunnel was surrounded by sand and clay with weak mechanical properties. Therefore, considering the fact that clay soils with very weak mechanical characteristics were not able to secure the tunnel stability during the tunnel excavation, pre-support UAM technique was deployed to reinforce the tunnel. The stability of the tunnel was crucial not only because of the engineering-related issues but also from the safety point of view, since the tunnel was exactly located beneath the residential area.

The UAM elements consisted of pipes, injected cement grout, and improved soil around the pipes (soilcrete) were simulated in the ABAQUS program. Forepoling pipes (wire elements) with 50 cm center-to-center installation distance were embedded at the tunnel crown. By injecting the cement grout to the forepoling borehole pipes a mixture of the surrounding soil and cement was formed, named soilcrete. Soilcrete elements were then modeled separately in the software to accurately simulate the UAM implementation. Considering the pipes total length (12 m) and the overlap length (3m) with the next set of them, the whole procedure of umbrella arch installation was consistently repeated after (12-3=9 m) of drilling. Figure 3 illustrates the simulated tunnel using the UAM after the 5<sup>th</sup> set of pipe installation and 42 m of tunnel excavation.

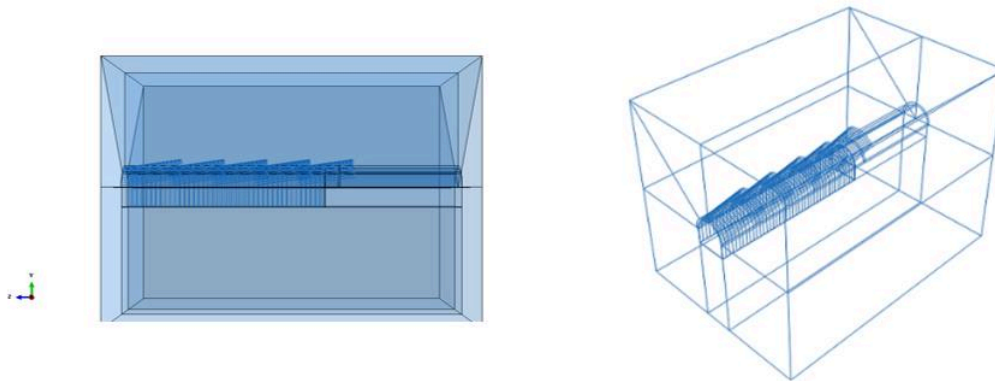


**Figure 3. Schematic view of UAM-reinforced tunnel, after 42 m of excavation.**

**Table 2. Mechanical Behaviors of Different Elements**

| Element                    | Soil         | Soilcrete    | Shotcrete               | Steel frame             | Pipes   |
|----------------------------|--------------|--------------|-------------------------|-------------------------|---------|
| <b>Mechanical Behavior</b> | Mohr-Coulomb | Mohr-Coulomb | Classic elastic-plastic | Classic elastic-plastic | Elastic |

**Table 3. Geotechnical Properties attributed to the Soil and Soilcrete**

| Parameter                          | Material |           | Unit              |
|------------------------------------|----------|-----------|-------------------|
|                                    | Soil     | Soilcrete |                   |
| Density ( $\rho$ )                 | 2000     | 2300      | Kg/m <sup>3</sup> |
| Young's modulus (E)                | 50       | 2600      | MPa               |
| Poisson's ratio ( $\nu$ )          | 0.3      | 0.3       | -                 |
| Cohesion (C)                       | 40       | 4200      | KPa               |
| Internal friction angle ( $\phi$ ) | 25       | 35        | Degree            |
| Dilation angle ( $\psi$ )          | 10       | 20        | Degree            |

### Mechanical Behaviors and Properties

Mohr-Coulomb model, as a relatively accurate and fast model (Beizaei et al. 2020), was assigned to the soil and soilcrete elements to better characterize these components. Mechanical behaviors of shotcrete, steel frames, and UAM pipes were defined as classic elastic-plastic, and

elastic, respectively. Deployed mechanical behavior models are summarized in Table 2. Additionally, several specimens were tested in the laboratory to characterize the properties of the soil and soilcrete elements. Obtained results from the laboratory test data, in terms of the geotechnical properties of the soil and jet grouted soilcrete at the vicinity of the tunnel are indicated in Table 3. Moreover, Table 4 indicates the material properties associated with the primary supporting system as well as the UAM pipes.

**Table 4. Mechanical Properties of the Supporting System Components**

| Parameter   | Density (Kg/m <sup>3</sup> ) | Young's modulus (GPa) | Poisson's ratio | 28-day strength (MPa) |
|-------------|------------------------------|-----------------------|-----------------|-----------------------|
| Shotcrete   | 2200                         | 26                    | 0.3             | 30                    |
| Steel frame | 7800                         | 200                   | 0.25            | -                     |
| UAM pipes   | 3200                         | 50                    | 0.35            | -                     |

### Boundary Conditions

Since boundary conditions play a critical role in FE modeling, attention should be paid to defining appropriate boundary conditions to assure a realistic model. Figure 4 shows different types of BCs defined in the simulation of the tunnel. ENCASTRE boundary condition was used at the bottom of the model to restrain the displacement and rotation in all directions. Moreover, two other BCs were defined in the FE models to restrict the displacement in the orthogonal direction to the indicated surfaces.

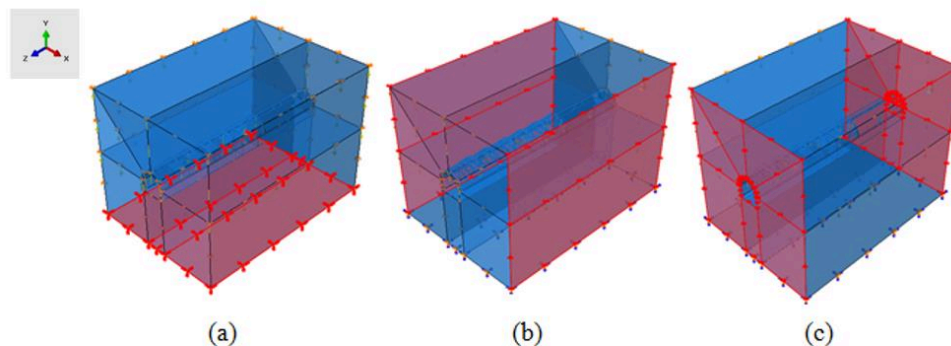


**Figure 4. Deployed boundary conditions in a) XZ plane ( $U_x = 0, U_y = 0, U_z = 0$ ), b) YZ plane ( $U_x = 0$ ), and c) XY plane ( $U_z = 0$ ).**

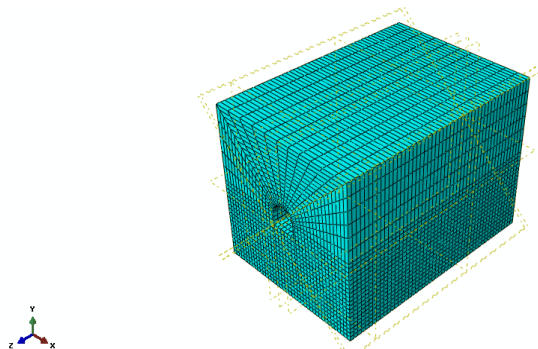


**Figure 5. Soil block meshing.**